catalysts

MDPI

Article

Mechanistic Insights into Fractal Kinetics and Cellulase Adsorption in the Saccharification of Avicel PH-101 and Pretreated Hemp Hurd

Stefano Gandolfi and Gianluca Ottolina *

Institute of Chemical Sciences and Technologies "Giulio Natta", National Research Council of Italy, via Mario Bianco 9, 20131 Milan, Italy; stefano.gandolfi@cnr.it

* Correspondence: gianluca.ottolina@cnr.it

Abstract

Background: The enzymatic saccharification of cellulose is governed by heterogeneous reaction environments that deviate from classical Michaelis–Menten behavior. Methods: Fractal kinetics were applied to describe the hydrolysis of microcrystalline cellulose (Avicel PH-101) and pretreated hemp hurds using Cellic CTec2. Optimal enzyme loading was first established on Avicel, and the influence of mixing regimes was evaluated. Results: Rotational agitation markedly improved hydrolysis efficiency. Organosolv-based pretreatments generated cellulose-enriched substrates that exhibited higher reactivity than Avicel, while redeposited lignin showed minimal inhibitory effects. Enzyme adsorption studies revealed substantial binding to lignocellulosic substrates, suggesting nonspecific interactions and crowding effects that influence kinetic parameters. Conclusions: Fractal coefficients *k* and *h* successfully captured differences in substrate accessibility and reactivity, demonstrating the suitability of fractal models for describing cellulose saccharification in complex solid–liquid systems. Organosolv pretreatment allows a high degree of saccharification, whereas redeposited lignin does not interfere with the enzymatic reaction.

Keywords: cellulose hydrolysis; fractal kinetics; enzyme adsorption; organosolv pretreatment; hemp hurds; Cellic CTec2; lignocellulosic biomass

1. Introduction

The enzymatic conversion of lignocellulosic biomass is a key step in developing sustainable technologies for producing biofuels and biochemicals. Cellulose, the most abundant organic polymer in nature, represents a strategic source of fermentable sugars; however, its high crystallinity and tight integration within the lignocellulosic matrix make its hydrolysis particularly challenging [1–4]. Lignin, a highly recalcitrant three-dimensional aromatic polymer, acts as both a physical and chemical barrier to cellulolytic enzymes, reducing hydrolysis efficiency through substrate shielding, steric hindrance, and non-productive adsorption [2,3]. The enzymatic hydrolysis of cellulose is catalyzed by cellulases, comprising mainly endoglucanases, exoglucanases, and β-glucosidases, which operate synergistically to degrade crystalline and amorphous cellulose structures [1]. However, their activity is strongly influenced by lignin, which competes for binding sites through nonspecific interactions that lower the effective concentration of active enzymes [2,5] and alter fundamental kinetic parameters such as V_{max} and K_m [3,6]. Because of its heterogeneous distribution and complex structure, lignin contributes to the nonlinear

Check for updates

Academic Editors: Xianxiang Liu, Shuolin Zhou and Xu Yang

Received: 27 February 2026
Revised: 12 March 2026
Accepted: 18 March 2026
Published: 1 April 2026

Copyright: © 2026 by the authors. Licensee MDPI, Basel, Switzerland. This article is an open access article distributed under the terms and conditions of the Creative Commons Attribution (CC BY) license.

character of cellulose hydrolysis kinetics, typically manifested by an initial rapid phase followed by a pronounced slowdown. These observations have motivated the development of kinetic models that go beyond the classical Michaelis–Menten formulation, incorporating concepts such as dynamic reactive surface area, substrate fragmentation, and lignin-induced enzyme deactivation [5].

Lignocellulosic biomass is composed mainly of cellulose (35–50%), hemicellulose (15–35%), and lignin (10–35%), tightly interconnected in a three-dimensional structure. The dense network of hydrogen bonds among cellulose chains generates highly ordered crystalline microfibrils embedded within hemicellulose and lignin, which protect the cellulose from microbial and chemical degradation [7]. Cellulose itself is a linear β-1,4-glucan with a degree of polymerization ranging from 800 to 10,000 units, forming hierarchical assemblies of microfibrils, macrofibrils, and fibers [7,8]. Hemicellulose is a branched, partially acetylated heteropolysaccharide composed of pentoses, hexoses, and related derivatives. It is generally less crystalline and more susceptible to hydrolysis [9], while lignin consists of a heterogeneous aromatic network derived from p-coumaryl, coniferyl, and sinapyl alcohols, conferring rigidity and resistance to degradation [10]. Biomass also contains extractives such as resins, terpenes, phenolics, and inorganic materials, although these components typically play a minor role in limiting cellulose conversion [11].

The bioconversion of lignocellulosic polysaccharides is of considerable industrial relevance, as both cellulose and hemicellulose can be depolymerized into fermentable sugars that serve as precursors for bio-based commodities and high-value chemicals. However, due to the recalcitrance of the native structure, pretreatment is required to disrupt the interactions among cellulose, hemicellulose, and lignin. Effective pretreatments must be cost-efficient, reduce recalcitrance, limit the formation of inhibitory compounds, and increase enzyme accessibility. Technologies available include physical, chemical, biological, and combined pretreatments [1,8,11]. The organosolv process enables efficient delignification using organic solvents and allows separation of biomass into cellulose, hemicellulose, and lignin fractions, although severe conditions can cause sugar degradation and formation of inhibitory compounds [12]. Pretreatment severity is often quantified via the combined severity factor, integrating temperature, reaction time, and pH [13].

Cellulases are produced by fungi, bacteria, archaea, insects, and plants. These organisms have evolved distinct strategies for cellulose degradation. Some microorganisms, such as *Trichoderma reesei*, secrete free cellulases; anaerobic bacteria, like *Clostridium,* assemble complexed cellulosomes; and others, including *Cytophaga hutchinsonii*, degrade cellulose through direct membrane-associated mechanisms [14,15]. Endoglucanases, exoglucanases, and β-glucosidases act synergistically to depolymerize cellulose to glucose. Endo- and exoglucanases can employ either inverting or retaining catalytic mechanisms and typically contain a catalytic domain, a carbohydrate-binding module, and a flexible linker. β-glucosidases hydrolyze cellobiose and short oligosaccharides, alleviating product inhibition. The synergistic action of cellulases is traditionally explained by the "*inchworm*" model, in which endoglucanases open amorphous regions, exoglucanases process chain ends, and β-glucosidases complete the conversion to glucose. However, additional complexities, including the importance of structural obstacles along cellulose fibrils and the contribution of accessory enzymes such as LPMO (AA9), a metal-dependent oxidoreductase that increases hydrolysis through oxidative cleavage, have been highlighted [16]. Commercial cellulase formulations still face limitations, such as non-productive binding to lignin, enzyme inactivation by pretreatment-derived inhibitors, and product inhibition. Consequently, industrial strategies increasingly rely on engineered enzyme cocktails or multi-organism blends to achieve balanced activity profiles.

The enzymatic hydrolysis of cellulose is inherently heterogeneous, influenced by substrate structure, surface properties, accessibility, and lignin content [17]. Because enzymes and substrates exist in separate phases, hydrolysis proceeds through a sequence of adsorption, catalysis, sliding, and desorption steps, each susceptible to inhibition or substrate evolution [18]. Diffusional phenomena, medium composition, and mixing conditions introduce additional complexity, leading to strong deviations from classical Michaelis–Menten kinetics [19]. To capture these dynamics, semiempirical fractal-based models have been proposed, particularly suited to reactions constrained spatially and affected by macromolecular crowding [20]. The restriction of enzyme mobility imposed by the fibrillar architecture of cellulose supports the use of such models to more accurately describe the kinetics of saccharification on solid substrates.

In this study, we applied fractal kinetic modeling to describe the enzymatic saccharification of microcrystalline cellulose and pretreated hemp hurds using Cellic CTec2 under heterogeneous reaction conditions. We systematically evaluated the effects of enzyme loading, mixing regime, substrate pretreatment, and enzyme adsorption on overall hydrolysis performance.

2. Results and Discussion

2.1. Determination of the Optimal Enzyme–Substrate Ratio for Avicel PH-101 Hydrolysis Reaction

Enzymatic hydrolysis of Avicel PH-101, a pure form of microcrystalline cellulose, was performed with different cellulase enzyme loadings at 50 °C and pH 4.8. The results are shown in Figure 1. Glucan conversion increases with increasing enzyme loading (expressed as filter paper units, a standardized measure of total cellulase activity) [21] and levels off at about 15–25 FPU/g_{Glucan}. Therefore, an enzyme loading of 20 FPU/g_{Glucan} was chosen as optimal for subsequent hydrolysis experiments.

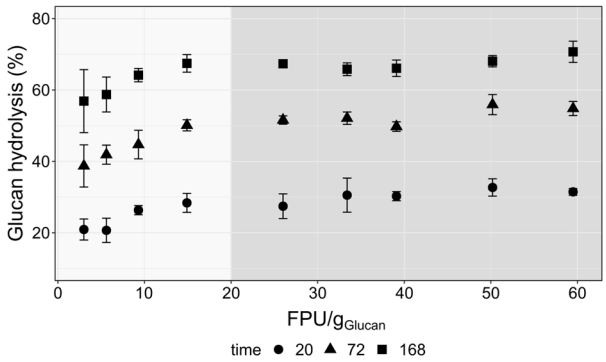

Figure 1. Effect of enzyme blend Cellic CTec2 loading in the hydrolysis of Avicel PH-101 at three different reaction times: 20, 72 and 168 h. Mean ± sd, n = 3.

2.2. Comparison of Enzymatic Hydrolysis Kinetics of Avicel PH-101 Cellulose

Cellulase enzymes exhibit processivity, a feature that implies their prolonged association with substrates and engagement in multiple catalytic cycles before detachment [22]. Enzymatic time-course hydrolysis of cellulose does not follow a first-order reaction, probably due to non-homogeneous and far from ideal solution conditions. Indeed, the best-fitting experimental data is usually obtained by applying fractal-like models [17,18,20]. Diffusion-controlled reactions that are constrained by geometry, as found in heterogeneous kinetics, can be described by reactions on fractal domains. Fractal-like reactions have several unique characteristics, including anomalous reaction orders and time-dependent reaction rate constants. These anomalies arise from the non-random distribution of reactants in low dimensions and may lead to segregation of reactants. In the fractal-like kinetic model used in this study, the reaction rate constant is replaced by a transient rate coefficient k_t

that decays over time as a function of two parameters: k, the rate constant, and h, the fractal exponent.

The enzymatic hydrolysis of Avicel PH-101 cellulose was performed at different enzyme loadings (FPU/g_{Glucan}) to evaluate its effect on the fractal parameters *k* and *h*. Experimental time courses (t) of enzymatic saccharification of the substrate (measured as glucose release or degree of conversion (DC)) are well described by the fractal model:

$$DC(\%) = 100 \cdot (1 - e\hat{}(-k \cdot (1 + (t\hat{}(1 - h) - 1)/(1 - h)))) \quad (1)$$

as shown by the superimposition of the model fit on the measured data in Figure S1 and the model parameters collected in Table S1. By plotting the calculated *k* and *h* values as a function of the enzyme loading (Figure 2), it can be seen that the transient rate coefficient *k* increases with increasing enzyme loading, whereas the fractal exponent *h* values appear more scattered around a constant value of 0.45 (average deviation ~7%). These observations partially agree with the results obtained by Wang and Feng in that the fractal exponent is more related to the nature of the substrate [17]. For diffusion-limited reactions that occur in fractal spaces, theory (and simulations) gives $h > 0$ and hence a transient rate coefficient *k*. For a reaction on a 1-D "*wire*", over an extended reaction time, *h* approaches 0.5. Since the *h* value is related to the fractal dimension, it can be considered independent of the enzyme loading with a value around 0.45, which is consistent with enzymatic kinetics in a segregated environment like cellulose [20].

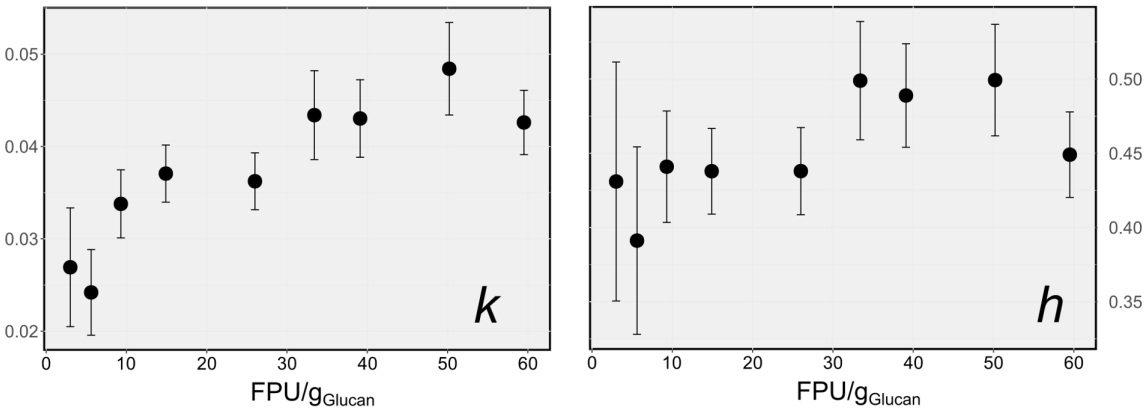

Figure 2. Effect of enzyme loading on fractal kinetic parameters *k* and *h* during the hydrolysis of Avicel PH-101. Estimate ± SE from Table S1.

Because of the heterogeneous reaction conditions, mixing of phases plays a crucial role in obtaining high saccharification levels. Most of the literature focuses on stirring control at high solid loading (liquid-to-solid ratio, LSR < 7) to reduce vessel volume and thus the associated capital and energy costs [23]. Compared to orbital agitation, the use of rotational mixing in a rotating reactor is known to improve the mass and heat transfer and minimize the enzyme deactivation induced by mechanical and thermal stress [24]. Moreover, rotating reactors allow for high solid loading [25]. Because of this, a switch was made to rotational agitation using a rotary drum reactor to evaluate the impact of different mixing regimes on the fractal kinetic parameters *k* and *h*. The previously determined optimal enzymatic concentration of 20 FPU/g_{Glucan} was used as a benchmark. As can be observed from Figure 3, enzymatic reactions performed under rotational mixing proceeded faster, leading to the achievement of high levels of saccharification in a shorter time. The highest hydrolysis achieved was about 83% after 168 h, which is 16% higher compared to the orbital stirring mode at a similar enzyme loading (Figure 1). However, as shown in Figure 3, increasing the amount of substrate in the reactor negatively affected the reaction

rate. This was further emphasized by decreasing the enzyme loading to 10 FPU/$g_{Biomass}$. The fitting of experimental data using Equation 1 allowed the *k* and *h* values to be obtained for this new reaction setting. Data analysis showed that, under orbital stirring, enzyme loading markedly influenced the transient rate coefficient *k*, which was almost double compared with orbital stirring under similar conditions, while the *h* value remained in the same range but increased with changes in LSR and enzyme loading (Table S2).

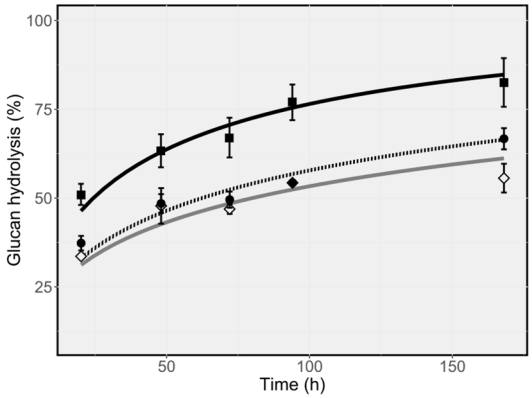

Figure 3. Effect of enzyme blend loading and LSR in the hydrolysis of Avicel PH-101 with rotational agitation of 10 rpm fitted using Equation (1). Black line, squares: 20 FPU/$g_{Biomass}$, LSR 10; dotted line, circles: 20 FPU/$g_{Biomass}$, LSR 5; gray line, diamonds: 10 FPU/$g_{Biomass}$, LSR 5. Mean ± sd, n = 3. At LSR 5, some values overlap. See Table S2.

2.3. Pretreatments and Analysis of Lignocellulosic Biomass Composition

Direct utilization of complex lignocellulosic matrices in the enzymatic hydrolysis of cellulose is hindered by the presence of hemicellulose and lignin. A pretreatment step is usually applied to break down the lignin structure and make cellulose accessible to enzymes during the hydrolysis step [26]. The lignocellulosic substrate used in this work (hemp hurds) was subjected to a series of preliminary treatments of destructuration to obtain different cellulose-enriched biomass. We focused on two pretreatment strategies: Soxhlet extraction and hydrothermal pulping in the presence of an organic solvent (organosolv). Specifically, four combinations of these pretreatments were applied to hemp hurds, resulting in four distinct biomasses: (i) Soxhlet–organosolv–Soxhlet (S–OS–S), (ii) Soxhlet–organosolv (S–OS), (iii) organosolv–Soxhlet (OS–S), and (iv) organosolv (OS). The lignin, xylan, and glucan content of each pretreated sample, as well as the untreated biomass, was determined, and the values are reported in Table S3. Total lignin was derived from the sum of acid-insoluble lignin (AIL) and acid-soluble lignin (ASL). For OS pretreatment, a CSF of ≈1.1 was chosen as a tradeoff between lignin removal and the enzymatic susceptibility of residual cellulose [12]. Methanol was used as a solvent for both Soxhlet and organosolv reactions, as it allows for the solubilization of oils, waxes and lignin. Moreover, methanol was found to be a good solvent for redeposited lignin on OS-pretreated biomass. Indeed, samples that did not undergo Soxhlet extraction after OS pretreatment (i.e., S–OS and OS) were found to contain a higher percentage of total lignin (Table S3). This finding is consistent with the fact that Soxhlet extraction carried out following OS allowed for the removal of lignin redeposited onto cellulose after the biomass had been returned to ambient temperature and pressure, which accounted for about 4% of total lignin. As expected, hydrothermal pretreatment efficiently allowed for the destructuration of the biomass, solubilizing the lignin and partially removing the hemicellulosic fraction because of the acidic reaction media, hence improving the enzymes' access to the cellulose fibers. Under the investigated pretreatment conditions, glucan percentage rose to 81.8% compared to 44% for the original material, while the hemicellulosic removal attained 36%. Soxhlet extraction did not significantly

affect the polysaccharidic fraction of the biomass, but, as previously discussed, it enabled removal of the redeposited lignin when applied after hydrothermal pretreatment.

2.4. Comparison of the Effects of Combined Chemical Pretreatments on Enzymatic Hydrolysis of Lignocellulosic Biomass

The time course of enzymatic hydrolysis results of pretreated lignocellulosic samples is reported in Figures S2 and S3, as well as in Tables S4 and S5. All reactions were conducted using a consistent LSR, agitation speed, and FPU dosage. Due to the different cellulose content of samples, depending on the pretreatment applied (Table S3), two sets of experiments were performed: one counting the whole biomass and another considering only the glucan content for the enzyme loading: 20 FPU/$g_{Biomass}$ or 20 FPU/g_{Glucan}, respectively. As for hydrolysis reactions using pure cellulose (Avicel PH-101), Equation 1 was used to fit experimental data points, giving satisfactory results in terms of correlation values and goodness-of-fit parameters. The kinetics curves obtained from pretreated samples are illustrated in Figure 4, and the hydrolysis of Avicel PH-101 is also included for reference. Interestingly, compared to the hydrolysis of Avicel PH-101-pretreated samples, faster hydrolysis has been reported in other studies, which could be attributed to the high crystallinity index of Avicel PH-101 [27]. It is well established that fungal cellulases hydrolyze amorphous cellulose at a significantly faster rate than the crystalline form [28].

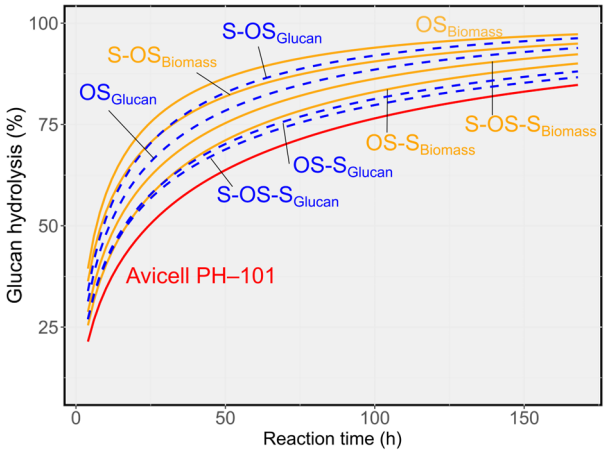

Figure 4. Enzymatic hydrolysis curve at LSR 10, rotational agitation 10 rpm of hemp hurds pretreated as OS, S–OS, OS–S and S–OS–S. 20 FPU/$g_{Biomass}$ (orange continuous line), 20 FPU/g_{Glucan} (blue dashed line). Avicel PH-101 red line. See Tables S4 and S5.

From a kinetic perspective, samples subjected to a final Soxhlet extraction exhibited a slower reaction rate, suggesting that this step is detrimental to enzymatic hydrolysis, even though it removes reprecipitated lignin. Indeed, it can be seen from Figure 4 that the impact of redeposited lignin from post-organosolv processing appears minimal on enzymatic hydrolysis. This is attributed to the high degree of delignification achieved or to the fact that this type of lignin does not hinder the activity of the enzymatic blend present in Cellic CTec2. Moreover, Soxhlet treatment before organosolv has practically no effect on lignin, cellulose and hemicellulose composition, as reported in Table S3.

However, while it has no effect on enzymatic hydrolysis, it can remove various organic compounds like oils and sterols [29]. The most favorable results are obtained without it (i.e., OS), suggesting that Soxhlet treatment is unnecessary for efficient cellulose hydrolysis. The values of k and h are reported in Tables S2, S4 and S5, indicating that the most efficient cellulose hydrolysis is achieved with high k and low h values (i.e., $OS_{Biomass}$ sample). A similar relationship between the k and h values and the hydrolysis rate of different pretreated lignocellulosic samples has been reported in [30]. Interestingly, the difference

between S-$OS_{Biomass}$ and S-OS_{Glucan} is negligible, even though different amounts of enzyme and starting materials (whole biomass vs. glucan fraction) were used. This suggests that factors beyond enzyme loading may govern the hydrolysis kinetics in these instances. In contrast, the main difference between OS_{Glucan} and $OS_{Biomass}$ is likely due to the different amounts of enzyme blend used in the two reactions. This result demonstrates that, for the studied lignocellulosic substrate, Soxhlet extraction for removal of oils, waxes, sterols, and redeposited lignin does not improve the rate of cellulose hydrolysis.

2.5. Adsorption of Cellic CTec2 Enzyme Blend on Avicel PH-101 Cellulose and Lignocellulosic Biomasses During Hydrolysis

Enzymatic hydrolysis of cellulose is a heterogeneous liquid-solid reaction, wherein the substrate exists in the insoluble solid phase, while the catalyst is soluble and resides in the liquid phase. This distinction necessitates that the enzyme adsorb onto the insoluble substrate and form cellulase-substrate complexes for initiating the hydrolysis reaction [27,31–35]. Therefore, tracking the adsorption of cellulolytic enzymes from the Cellic CTec2 mixture onto cellulose during the reaction by assessing the amount of enzyme bound to the substrate is crucial for comprehending the reaction's progress.

To this aim, protein quantification was employed using fluorescence intensity analysis, leveraging the propensity of tryptophan residues in proteins to emit fluorescence upon excitation at 280 nm, followed by fluorescence emission at 348 nm. Through this approach, a calibration curve was constructed, enabling the determination of the free enzyme concentration in solution at each sampling time; glucose did not give quenching. Notably, the Cellic CTec2 enzyme mixture employed in this study encompasses not only cellulase but also other enzymatic activities, such as β-glucosidase, which are integrated into the overall free enzyme concentration. However, it is essential to recognize that cellulase and certain hemicellulolytic enzymes directly bind the residual cellulose and hemicellulose polymers, while other enzymes in the mixture, particularly β-glucosidases, operate on the liberated cellobiose residues in the liquid phase. Nevertheless, the possibility of nonspecific adsorption with biomass cannot be excluded.

The rapid adsorption and binding of cellulases to cellulose are well established. Therefore, to study the kinetics of this process, experiments are typically conducted at low or ambient temperature [33,36,37]. In contrast, in this study, fluorescence measurements are taken under the optimal conditions for cellulose hydrolysis. Within the initial five minutes of the reaction, 30% of the Cellic CTec2 enzyme mixture binds to Avicel PH-101. This percentage gradually increases until it reaches a plateau of around 45% after approximately 50 h of reaction (Figure 5a).

At this point in the hydrolytic reaction, an equilibrium has likely been established between the enzymes that have adsorbed onto the cellulose and those that remain in the solution, resulting in an almost stable percentage of bound enzyme. Similar behavior occurs for hemp hurds. However, it is remarkable that the bound fraction of the Cellic CTec2 enzyme mixture stabilizes at approximately 80% for all four pretreated samples (Figure 5a). The variation in the percentage of enzymes bound, from 45 to 80%, could be attributed to the heterogeneous composition of the biomass, which not only contains cellulose but also various other components such as lignin and residual hemicellulose (Table S3). Interestingly, the amount of adsorbed enzymes shows minimal dependence on the residual lignin content, suggesting a nonspecific adsorption. The conversion of cellulose to glucose leads to a depletion over time that could affect the hydrolysis rate only when its concentration becomes limiting. However, these enzymes are processive, meaning they can perform multiple rounds of catalysis on cellulose before releasing it. Furthermore, it has been recognized that the dissociation from cellulose is considered the rate-limiting step in the absence of other hindrances caused by the structure of the biomass itself, such as the

presence of other biomolecules like lignin [34,38,39]. Figure 5b shows the amount of bound enzymes as a function of reaction progress. This reveals that the amount of enzyme bound to the biomass steadily increases, not only for hemp hurds containing residual lignin and hemicellulose, but also for Avicel PH-101. This high enzyme concentration may hinder the enzyme's processive movement, which is crucial for catalysis. This congestion could then lead to a decrease in reaction rate. As for Avicel, it is interesting to note that the amount of enzyme bound to cellulose continues to increase to a value well above 100 mg/$g_{Biomass}$, five-fold the initial amount. A similar trend has been observed for pretreated hemp hurds. However, because a substantial amount of lignin is still present, it can be argued that some of the enzymes bind to it in a nonspecific manner, reducing the actual amount available on the cellulosic portion that facilitates cellulase mobility and, therefore, cellulose hydrolysis. These observations could explain that despite a lower fractal value *h* obtained for Avicel PH-101, the reaction rate constant *k* is lower compared to the values obtained for pretreated hemp hurds, which leads to generally higher saccharification levels for the latter, suggesting a crowding effect on the substrate surface at high conversion yields.

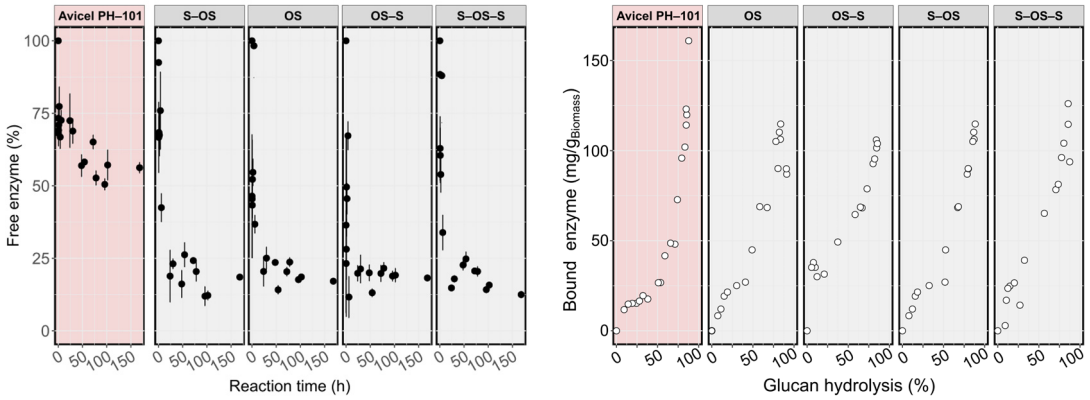

Figure 5. (**a**) Fluorescence determination of free enzyme adsorption at 20 FPU/g_{Glucan} of Avicel PH-101 and hemp hurds, S–OS, OS, OS–S and S–OS–S at LSR 10 with rotational agitation. Enzyme concentration, 100% at t = 0, as follows: Avicel PH-1013.98; S–OS 3.12; OS 2.94; OS–S 3.17; S–OS–S 3.27 mg/mL. (**b**) Enzyme bound to the biomass, Avicel PH-101, and pretreated hemp hurds as a function of the reaction progress, measured by glucan hydrolysis (%) at 20 FPU/$g_{Biomass}$.

3. Materials and Methods

3.1. Raw Materials, Enzymes, and Chemicals

Hemp hurds, variety Carmagnola (Assocanapa, Carmagnola, Italy), were sorted and milled as previously described [29]. Avicel PH-101 and Cellic CTec2 enzyme mixture were purchased from Merck (Darmstadt, Germany), and activity was measured as filter paper unit (FPU) [21]. All chemicals were used as received and were of analytical grade.

3.2. Determination of the Optimal Enzyme–Substrate Ratio for Avicel PH-101 Hydrolysis Reaction

The enzymatic hydrolysis of pure microcrystalline cellulose (Avicel PH-101) was carried out using the Cellic CTec2 enzyme mixture. The reaction was carried out in 5 mL vials in an orbital shaker at 50 °C and 100 rpm for 168 h. In all experiments, 0.05 M sodium citrate buffer at pH 4.8 and 500 mg Avicel PH-101 were used. Kinetic reactions were set up with different concentrations of enzyme mixture (3–60 FPU/g_{Glucan}) in triplicate and sampled at 20, 48, 72, 94, and 168 h. Quantification of glucose was carried out by HPLC using a Rezex RHM-Monosaccharide H+ (8%), an ion exclusion column (Phenomenex, Torrance, CA, USA) at 85 °C and an evaporative light-scattering ELS-2041 detector (Jasco, Hachioji, Japan) with ultrapure water as the mobile phase, with a flow rate of 0.6 mL/min,

were used. The linearity obtained between the signal intensity and the corresponding sugar concentrations was in the range of 0.10–0.55 mg/mL with a good correlation coefficient (0.9990). The limit of detection was 0.01 mg/mL, and the limit of quantification was 0.04 mg/mL. Experimental hydrolysis time courses were fitted according to the fractal model as described in Equation (1) [17].

3.3. Comparison of Enzymatic Hydrolysis Kinetics of Avicel PH-101 Cellulose

Three different kinetic experiments were performed in triplicate to assess enzymatic hydrolysis reaction conditions, as reported in Table 1. Experiments were performed in 2 mL vials using a reaction volume of 1.5 mL and kept at 50 °C under agitation at 10 rpm using a tube roller (Thermo Fisher Scientific Inc., Waltham, MA, USA). For all the experimental sets, 0.05 M sodium citrate buffer at pH 4.8 was used. Glucose release was monitored by HPLC through sampling reactions after 20, 48, 72, 94 and 168 h.

Table 1. Experimental conditions of Avicel PH-101 enzymatic hydrolysis reaction.

#	Avicel PH-101	Cellic CTec2		LSR
	mg	FPU	$FPU/g_{Biomass}$	
1	150	3	20	10
2	300	6	20	5
3	300	3	10	5

3.4. Pretreatments and Analysis of Lignocellulosic Biomass Composition

The organosolv hydrothermal pretreatment (OS) of lignocellulosic substrate was performed and analyzed according to Gandolfi [12,29]. The pretreatment combined severity factor (CSF) [13], calculated by Equation (2), was set to ≈1.1, and an LSR of 10 was used for all experiments.

$$CSF = \log(t \cdot e\hat{}((T - T_{ref})/14.75)) - pH \quad (2)$$

where t is the pretreatment reaction time in minutes; T is the pretreatment hydrolysis temperature (°C); T_{ref} is the reference temperature, which corresponds to 100 °C; and pH is the value of the liquid phase after the pretreatment.

3.5. Soxhlet Extraction

Before and/or after the pretreatment, the biomass was subjected to Soxhlet extraction in methanol for about 20 cycles.

3.6. Comparison of the Effects of Combined Chemical Pretreatments on Enzymatic Hydrolysis of Lignocellulosic Biomass

Four different pretreatments were applied to hemp hurds lignocellulosic biomass before enzymatic hydrolysis: S–OS–S, S–OS, OS–S, and OS. Enzymatic reactions were performed in triplicate, as described above, using an enzyme loading of 20 $FPU/g_{Biomass}$ or 20 FPU/g_{Glucan} and an LSR of 10.

3.7. Adsorption of Cellic CTec2 Enzyme Mixture on Avicel PH-101 Cellulose and Lignocellulosic Biomass During Hydrolysis

Four different pretreated hemp hurd samples (S–OS–S, S–OS, OS–S, and OS) and Avicel PH-101 were subjected to enzymatic hydrolysis in triplicate, as already described, using an enzyme loading of 20 FPU/g_{Glucan} and LSR 10. Reactions were monitored for 216 h. Samples of the liquid fraction were withdrawn regularly for protein concentration analysis (see below) and glucose release by HPLC. Spectrofluorimetric quantification of protein was performed after sample dilution with distilled water. The fluorescence intensity

was read at emission wavelengths between 260 and 400 nm after excitation at 280 nm. The linearity obtained between the fluorescence emission and protein concentrations was in the range of 5–11 µg/mL with a good correlation coefficient (0.9972). The limit of detection was 0.4 µg/mL, and the limit of quantification was 1.2 µg/mL. The protein concentration of Cellic CTec2 was previously determined according to the BCA protein assay kit (Merck) as 270 ± 10 mg/mL.

3.8. Kinetic Calculation and Statistical Analysis

Kinetic calculation and statistical analysis were performed in the R environment (version 4.5.2). Equation (1) was used to describe the degree of conversion (DC) of cellulose to glucose units in a time-course reaction [17], where k is the transient rate coefficient, h is the fractal dimension, and t is the time.

4. Conclusions

The good fitness of the fractal kinetic model applied to the enzymatic saccharification of cellulose and pretreated hemp hurd experimental data indicates that it is suitable to describe the complex profile of these non-homogeneous reactions. The kinetic parameter k is a good descriptor for substrate reactivity, whereas the fractal exponent h appears to be more related to enzyme accessibility. Enzymatic hydrolysis results demonstrate that OS pretreatment allows for a high degree of saccharification. Rotational agitation markeI confirmdly improves hydrolysis efficiency compared with orbital agitation. Interestingly, it has been shown that redeposited lignin from organosolv pretreatment does not interfere with the enzymatic reaction.

Supplementary Materials: The following supporting information can be downloaded at https://www.mdpi.com/article/10.3390/catal16040304/s1, Figure S1: Fitting of the experimental data of Avicel PH-101 cellulose hydrolysis using the fractal kinetic model; Figure S2: Fitting of the experimental data of hemp hurds hydrolysis at 20 FPU/$g_{Biomass}$ OS, S–OS, OS–S and S–OS–S using the fractal kinetic model; Figure S3: Fitting of the experimental data of hemp hurd hydrolysis at 20 FPU/g_{Glucan} OS, S–OS, OS–S and S–OS–S using the fractal kinetic model. In dark gray is reported the predicted interval (PI); Table S1: Nonlinear regression models of the experimental hydrolysis of Avicel PH-101 cellulose with orbital stirring; Table S2: Nonlinear regression models of the experimental hydrolysis of Avicel PH-101 cellulose with rotational stirring; Table S3: Chemical composition of hemp hurds OS, S–OS, OS–S and S–OS–S before and after pretreatments in weight percentage on a dry basis; Table S4: Nonlinear regression models of the experimental hydrolysis of hemp hurds at 20 FPU/$g_{Biomass}$ OS, S–OS, OS–S and S–OS–S with rotational stirring; Table S5: Nonlinear regression models of the experimental hydrolysis of hemp hurds at 20 FPU/g_{Glucan} OS, S–OS, OS–S and S–OS–S with rotational stirring.

Author Contributions: Conceptualization, S.G. and G.O.; methodology, G.O.; software, G.O.; validation, S.G. and G.O.; formal analysis, G.O.; investigation, S.G. and G.O.; resources, G.O.; data curation, G.O.; writing—original draft preparation, S.G.; writing—review and editing, S.G. and G.O.; visualization, G.O.; supervision, G.O.; project administration, G.O.; funding acquisition, G.O. All authors have read and agreed to the published version of the manuscript.

Funding: This work was supported by the MICS (Made in Italy—Circular and Sustainable) Extended Partnership and received funding from the European Union Next-Generation EU (PIANO NAZIONALE DI RIPRESA E RESILIENZA (PNRR)—MISSIONE 4 COMPONENTE 2, INVESTIMENTO 1.3—D.D. 1551.11-10-2022, PE00000004, CUP B53C22004100001). This manuscript reflects only the authors' views and opinions; neither the European Union nor the European Commission can be considered responsible for them.

Data Availability Statement: Further data besides those already reported in the article are available on request.

Acknowledgments: The author thanks Donatella Varinelli for skillful technical assistance and Benedetta Cordero di Montezemolo for administrative assistance.

Conflicts of Interest: The authors declare no conflicts of interest.

References

1. Kumar, P.; Barrett, D.M.; Delwiche, M.J.; Stroeve, P. Methods for Pretreatment of Lignocellulosic Biomass for Efficient Hydrolysis and Biofuel Production. *Ind. Eng. Chem. Res.* **2009**, *48*, 3713–3729. [CrossRef]
2. Berlin, A.; Balakshin, M.; Gilkes, N.; Kadla, J.; Maximenko, V.; Kubo, S.; Saddler, J. Inhibition of Cellulase, Xylanase and β-Glucosidase Activities by Softwood Lignin Preparations. *J. Biotechnol.* **2006**, *125*, 198–209. [CrossRef]
3. Rahikainen, J.; Mikander, S.; Marjamaa, K.; Tamminen, T.; Lappas, A.; Viikari, L.; Kruus, K. Inhibition of Enzymatic Hydrolysis by Residual Lignins from Softwood—Study of Enzyme Binding and Inactivation on Lignin-Rich Surface. *Biotechnol. Bioeng.* **2011**, *108*, 2823–2834. [CrossRef]
4. Yoo, C.G.; Meng, X.; Pu, Y.; Ragauskas, A.J. The Critical Role of Lignin in Lignocellulosic Biomass Conversion and Recent Pretreatment Strategies: A Comprehensive Review. *Bioresour. Technol.* **2020**, *301*, 122784. [CrossRef]
5. Santos, D.; Siqueira, J.G.W.; Silva, M.G.L.d.; Donato, M.; Silva, G.d.; Pratto, B.; Albuquerque, A.A.; Dutra, E.D.; Sonego, J.L.S. Enzymatic Hydrolysis of Lignocellulosic Biomass: Structural Features, Process Aspects, Kinetics, and Computational Tools. *Biomass* **2026**, *6*, 13. [CrossRef]
6. Fang, L.; Lai, C.; Hua, Q.; Wang, P.; Huang, C.; Ling, Z.; Yong, Q. Lignin-Associated Factors Impede Enzymatic Hydrolysis of Hydrothermally Pretreated Birch and Poplar Wood. *Ind. Crops Prod.* **2025**, *226*, 120704. [CrossRef]
7. Zamani, A. Introduction to Lignocellulose-Based Products. In *Lignocellulose-Based Bioproducts*; Karimi, K., Ed.; Springer International Publishing: Cham, Switzerland, 2015; pp. 1–36, ISBN 978-3-319-14033-9.
8. Shafiei, M.; Kumar, R.; Karimi, K. Pretreatment of Lignocellulosic Biomass. In *Lignocellulose-Based Bioproducts*; Karimi, K., Ed.; Springer International Publishing: Cham, Switzerland, 2015; pp. 85–154, ISBN 978-3-319-14033-9.
9. Huang, L.-Z.; Ma, M.-G.; Ji, X.-X.; Choi, S.-E.; Si, C. Recent Developments and Applications of Hemicellulose From Wheat Straw: A Review. *Front. Bioeng. Biotechnol.* **2021**, *9*, 690773. [CrossRef] [PubMed]
10. Ali, S.; Rani, A.; Dar, M.A.; Qaisrani, M.M.; Noman, M.; Yoganathan, K.; Asad, M.; Berhanu, A.; Barwant, M.; Zhu, D. Recent Advances in Characterization and Valorization of Lignin and Its Value-Added Products: Challenges and Future Perspectives. *Biomass* **2024**, *4*, 947–977. [CrossRef]
11. Karimi, K.; Shafiei, M.; Kumar, R. Progress in Physical and Chemical Pretreatment of Lignocellulosic Biomass. In *Biofuel Technologies: Recent Developments*; Gupta, V.K., Tuohy, M.G., Eds.; Springer: Berlin/Heidelberg, Germany, 2013; pp. 53–96, ISBN 978-3-642-34519-7.
12. Gandolfi, S.; Ottolina, G.; Consonni, R.; Riva, S.; Patel, I. Fractionation of Hemp Hurds by Organosolv Pretreatment and Its Effect on Production of Lignin and Sugars. *ChemSusChem* **2014**, *27*, 7186–7189. [CrossRef] [PubMed]
13. Lee, J.-W.; Jeffries, T.W. Efficiencies of Acid Catalysts in the Hydrolysis of Lignocellulosic Biomass over a Range of Combined Severity Factors. *Bioresour. Technol.* **2011**, *102*, 5884–5890. [CrossRef]
14. Yan, S.; Xu, Y.; Yu, X.-W. From Induction to Secretion: A Complicated Route for Cellulase Production in *Trichoderma reesei*. *Bioresour. Bioprocess.* **2021**, *8*, 107. [CrossRef]
15. Song, W.; Geng, S.; Qi, Q.; Lu, X. Ugd Is Involved in the Synthesis of Glycans of Glycoprotein and LPS and Is Important for Cellulose Degradation in *Cytophaga hutchinsonii*. *Microorganisms* **2025**, *13*, 395. [CrossRef]
16. Munzone, A.; Eijsink, V.G.H.; Berrin, J.-G.; Bissaro, B. Expanding the Catalytic Landscape of Metalloenzymes with Lytic Polysaccharide Monooxygenases. *Nat. Rev. Chem.* **2024**, *8*, 106–119. [CrossRef]
17. Wang, Z.; Feng, H. Fractal Kinetic Analysis of the Enzymatic Saccharification of Cellulose under Different Conditions. *Bioresour. Technol.* **2010**, *101*, 7995–8000. [CrossRef] [PubMed]
18. Bansal, P.; Hall, M.; Realff, M.J.; Lee, J.H.; Bommarius, A.S. Modeling Cellulase Kinetics on Lignocellulosic Substrates. *Biotechnol. Adv.* **2009**, *27*, 833–848. [CrossRef] [PubMed]
19. Xu, F.; Ding, H. A New Kinetic Model for Heterogeneous (or Spatially Confined) Enzymatic Catalysis: Contributions from the Fractal and Jamming (Overcrowding) Effects. *Appl. Catal. A-Gen.* **2007**, *317*, 70–81. [CrossRef]
20. Kopelman, R. Fractal Reaction Kinetics. *Science* **1988**, *241*, 1620–1626. [CrossRef]
21. Adney, B.; Baker, J. *Measurement of Cellulase Activities: Laboratory Analytical Procedure (LAP)*; Issue Date: 08/12/1996; Technical Report; NREL: Golden, CO, USA, 2008.
22. Breyer, W.A.; Matthews, B.W. A Structural Basis for Processivity. *Protein Sci.* **2001**, *10*, 1699–1711. [CrossRef]
23. Jiang, X.; Zhai, R.; Jin, M. Increased Mixing Intensity Is Not Necessary for More Efficient Cellulose Hydrolysis at High Solid Loading. *Bioresour. Technol.* **2021**, *329*, 124911. [CrossRef]

24. Bhagia, S.; Dhir, R.; Kumar, R.; Wyman, C.E. Deactivation of Cellulase at the Air-Liquid Interface Is the Main Cause of Incomplete Cellulose Conversion at Low Enzyme Loadings. *Sci. Rep.* **2018**, *8*, 1350. [CrossRef]
25. Volynets, B.; Ein-Mozaffari, F.; Dahman, Y. Biomass Processing into Ethanol: Pretreatment, Enzymatic Hydrolysis, Fermentation, Rheology, and Mixing. *Green Process. Synth.* **2017**, *6*, 1–22. [CrossRef]
26. Mankar, A.R.; Pandey, A.; Modak, A.; Pant, K.K. Pretreatment of Lignocellulosic Biomass: A Review on Recent Advances. *Bioresour. Technol.* **2021**, *334*, 125235. [CrossRef]
27. Monschein, M.; Reisinger, C.; Nidetzky, B. Enzymatic Hydrolysis of Microcrystalline Cellulose and Pretreated Wheat Straw: A Detailed Comparison Using Convenient Kinetic Analysis. *Bioresour. Technol.* **2013**, *128*, 679–687. [CrossRef]
28. Lynd, L.R.; Weimer, P.J.; van Zyl, W.H.; Pretorius, I.S. Microbial Cellulose Utilization: Fundamentals and Biotechnology. *Microbiol. Mol. Biol. Rev.* **2002**, *66*, 506–577. [CrossRef]
29. Gandolfi, S.; Ottolina, G.; Riva, S.; Fantoni, G.P.; Patel, I. Complete Chemical Analysis of Carmagnola Hemp Hurds and Structural Features of Its Components. *BioResources* **2013**, *8*, 2641–2656. [CrossRef]
30. Wojtusik, M.; Vergara, P.; Villar, J.C.; Ladero, M.; García-Ochoa, F. Enzymatic Hydrolysis of Several Pretreated Lignocellulosic Biomasses: Fractal Kinetic Modelling. *Bioresour. Technol.* **2020**, *318*, 124050. [CrossRef] [PubMed]
31. Peciulyte, A.; Karlström, K.; Larsson, P.T.; Olsson, L. Impact of the Supramolecular Structure of Cellulose on the Efficiency of Enzymatic Hydrolysis. *Biotechnol. Biofuels* **2015**, *8*, 56. [CrossRef] [PubMed]
32. Rommi, K.; Holopainen, U.; Pohjola, S.; Hakala, T.K.; Lantto, R.; Poutanen, K.; Nordlund, E. Impact of Particle Size Reduction and Carbohydrate-Hydrolyzing Enzyme Treatment on Protein Recovery from Rapeseed (*Brassica rapa* L.) Press Cake. *Food Bioprocess Technol.* **2015**, *8*, 2392–2399. [CrossRef]
33. Zheng, Y.; Zhang, R.; Pan, Z. Investigation of Adsorption Kinetics and Isotherm of Cellulase and β-Glucosidase on Lignocellulosic Substrates. *Biomass Bioenergy* **2016**, *91*, 1–9. [CrossRef]
34. Vermaas, J.V.; Kont, R.; Beckham, G.T.; Crowley, M.F.; Gudmundsson, M.; Sandgren, M.; Ståhlberg, J.; Väljamäe, P.; Knott, B.C. The Dissociation Mechanism of Processive Cellulases. *Proc. Natl. Acad. Sci USA* **2019**, *116*, 23061–23067. [CrossRef] [PubMed]
35. Zajki-Zechmeister, K.; Kaira, G.S.; Eibinger, M.; Seelich, K.; Nidetzky, B. Processive Enzymes Kept on a Leash: How Cellulase Activity in Multienzyme Complexes Directs Nanoscale Deconstruction of Cellulose. *ACS Catal.* **2021**, *11*, 13530–13542. [CrossRef]
36. Liu, W.; Ren, Q.; Wu, R.; Wang, B.; Hu, Y.; Hou, Q.; Ni, Y. Insight on Adsorption of Cellulase on Wet Ground Corncob Residues and Its Evaluation by Multivariate Linear Analysis. *Bioresour. Technol.* **2020**, *318*, 124107. [CrossRef] [PubMed]
37. Wang, Q.q.; Zhu, J.y.; Hunt, C.g.; Zhan, H.y. Kinetics of Adsorption, Desorption, and Re-Adsorption of a Commercial Endoglucanase in Lignocellulosic Suspensions. *Biotechnol. Bioeng.* **2012**, *109*, 1965–1975. [CrossRef] [PubMed]
38. Cruys-Bagger, N.; Elmerdahl, J.; Praestgaard, E.; Tatsumi, H.; Spodsberg, N.; Borch, K.; Westh, P. Pre-Steady-State Kinetics for Hydrolysis of Insoluble Cellulose by Cellobiohydrolase Cel7A. *J. Biol. Chem.* **2012**, *287*, 18451–18458. [CrossRef] [PubMed]
39. Kari, J.; Olsen, J.; Borch, K.; Cruys-Bagger, N.; Jensen, K.; Westh, P. Kinetics of Cellobiohydrolase (Cel7A) Variants with Lowered Substrate Affinity. *J. Biol. Chem.* **2014**, *289*, 32459–32468. [CrossRef]

Disclaimer/Publisher's Note: The statements, opinions and data contained in all publications are solely those of the individual author(s) and contributor(s) and not of MDPI and/or the editor(s). MDPI and/or the editor(s) disclaim responsibility for any injury to people or property resulting from any ideas, methods, instructions or products referred to in the content.